Errata: *Surface instabilities of constrained elastomeric layers subject to electro-static stressing* by J. W. Hutchinson, J. Mech. Phys. Solids 153 (2021) 104462.

J. W. Hutchinson[1], R. Huang[2] and C. M. Landis[2,3]

[1]School of Engineering and Applied Sciences, Harvard University, Cambridge, MA
[2]Dept. of Aerospace Engineering and Engineering Mechanics, University of Texas, Austin, TX
[3]Oden Institute for Computational Engineering and Science, University of Texas, Austin, TX

Thanks to the help of the coauthors of this erratum (RH & CML), it has been possible to identify and correct an error in the bifurcation analysis of the first author (JWH) for the constrained layer problems addressed in the paper cited above. The error is not obvious, and the results for this problem are anticipated to be important for subsequent work on electro-mechanical instabilities. Therefore, this note briefly presents the corrected results along with discussion to make it less likely the error will be repeated. The error in the bifurcation analysis propagates throughout the post-bifurcation and imperfection-sensitivity analysis in the paper cited above giving rise to additional changes. Corrections to the post-buckling behavior are made in the Supplementary Materials accompanying this erratum with one figure summarizing selected results included below.

The said paper (Hutchinson, 2021) considered strictly incompressible neo-Hookean materials (and the Gent extension). An infinite layer is subject to an equi-biaxial pre-stretch, λ_0, prior to being bonded to a rigid substrate (see Fig. 1a). In the pre-bifurcation state the layer is uniform with thickness h. In Problem I, the top and bottom surfaces of layer are conducting with a voltage V_0 imposed across them. The layer is dielectric with permittivity ε. In Problem II, a voltage difference V_0 is imposed between a rigid conducting electrode located a distance h above the conducting top surface of the layer. In II, the medium between the conducting surfaces (vacuum, gas or liquid) has permittivity ε. In the notation and nondimensionalization of the paper, with $(x, y) = k(x_1, x_2)$, $k = 2\pi / \ell$ and ℓ as the wavelength, the periodic displacements of the plane strain bifurcation modes of the layer have the separated form:
$(u_1, u_2) = \ell(U(y)\sin(kx), V(y)\cos(kx))$. The corrected functional governing bifurcation for the Gent generalization of the incompressible neo-Hookean material is

$$\frac{\Delta\Psi_2}{\mu\ell^2} = \frac{\pi}{2}\int_{-y_B}^{0} \frac{1}{\omega_0}\left\{\lambda_0^2\left(U^2+V^2\right)+\lambda_0^{-4}\left(U'^2+V'^2\right)-2\lambda_0^{-4}\left(UV\right)'+\frac{2}{\omega_0 J_L}\left(\lambda_0^2 U+\lambda_0^{-4}V'\right)^2\right\}dy$$
$$-\frac{\pi}{2}\left[\Omega\,\mathrm{cotanh}(y_B)-\frac{2\pi\gamma}{\mu\ell}\right]V(0)^2 \tag{1}$$

with μ as the ground state shear modulus, γ as the surface energy, J_L as the Gent stiffening parameter, $(\ )' = d(\ )/dy$, $\omega_0 = 1 - (2\lambda_0^2 + \lambda_0^{-4} - 3)/J_L$ and $y_B = 2\pi h / \ell$. The dimensionless

eigenvalue parameter determining the voltage at bifurcation is $\Omega = (\varepsilon/\mu)(V_0/h)^2$. The incompressibility constraint, $V' + U = 0$, must be enforced using a Lagrange multiplier. In the limit $J_L \to \infty$ the neo-Hookean material is obtained. The functional is applicable to the bifurcation in both Problems I and II.

The error in the bifurcation functionals listed in Hutchinson (2021), i.e., (3.4), (4.1) and (4.4), is a single term uniquely identified by the factor $\tau\Omega$ (with $\tau = 1$ for I and $\tau = -1$ for II). Although the form is somewhat different, (1) is equivalent to the functional (4.4) in the original paper when the term $\tau\Omega$ is deleted. The terms in (1) comprise all the quadratic changes in the elastic, electro-static and surface energies making up the free energy of the system. The term in the original paper involving $\tau\Omega$ arises from the hydrostatic stress in the pre-bifurcation state of the layer. It can be eliminated from the integral over the layer and expressed as a surface contribution to the energy functional, as it has in (4.4) of the paper. The term is not a contribution to the strain energy in layer, which depends on the deformation but not the hydrostatic stress. The surface contribution of this term is not compatible with the electro-static traction changes generated by the bifurcation displacements. The validity of this argument did not come directly. We became convinced there was an error in the critical voltage for the incompressible material when independent analyses first conducted by RH and CML for bifurcation in Problem I for compressible neo-Hookean materials clearly approached a limit different from that given in the paper when calculations for nearly incompressible materials were carried out. Here we will provide the results from one such calculation focusing on Problem I with no pre-stretch ($\lambda_0 = 1$) and for the short wavelength limit valid when ℓ/h is sufficiently small.

The analysis described next employs a version of an isotropic, finite strain compressible material whose incompressible limit coincides with the neo-Hookean material, as described by Boyce and Arruda (1990), c.f., their equations (35) and (36). The compressible analysis is carried out for Problem I in the reference configuration prior to the application of the voltage V_0. Coordinates in the reference configuration are denoted X_I, and those in the current configuration are denoted x_i. The deformation gradient is $F_{iJ} = \frac{\partial x_i}{\partial X_J} = x_{i,J}$. The nominal electric field is $E_I = \frac{\partial \phi}{\partial X_I} = \phi_{,I}$, where ϕ is the electric potential. The true electric field is $e_i = \frac{\partial \phi}{\partial x_i} = \phi_{,i} = \frac{\partial \phi}{\partial X_J}\frac{\partial X_J}{\partial x_i} = F_{Ji}^{-1}E_J$. The form of the free energy used in this work is,

$$W = \frac{\mu}{2}\left(F_{iJ}F_{iJ} - 3\right) - \mu\ln J + \frac{\lambda}{2}(J-1)^2 - \frac{\epsilon}{2}JF_{Ki}^{-1}F_{Li}^{-1}E_K E_L \tag{2}$$

Here, μ and λ are the usual Lamé parameters when the material is subjected to infinitesimal deformation, ϵ is the dielectric permittivity, and $J = \det(F_{iJ})$ is the determinant of the deformation gradient. The analysis was also performed for a second compressible form shown

in Fig. 1b, where the bulk modulus κ is related to the Lamé parameters as, $\kappa = \lambda + 2\mu/3$. We present the details for the form in Eq. (2) because of its simpler analytic solution. The governing equations of equilibrium and charge balance, i.e. Gauss' law, are given as,

$$P_{Ji,J} = 0 \quad \text{and} \quad D_{I,I} = 0 \tag{3}$$

where $P_{Ji} = \frac{\partial W}{\partial F_{iJ}}$ is the first Piola-Kirchhoff stress, and $D_I = -\frac{\partial W}{\partial E_I}$ is the nominal electric displacement.

We look for perturbed solutions about a homogeneous state given by,

$$x_i = \delta_{iJ}X_J + \varepsilon_0\delta_{i2}X_2 + \alpha u_i(X_1, X_2) \tag{4}$$

$$\phi = \frac{V_0}{h}(X_2 + h) + \alpha\varphi(X_1, X_2) \tag{5}$$

where h is the film thickness in the reference state, V_0 is the voltage applied to the top surface at $X_2 = 0$, ε_0 is the film strain in the X_2 direction at the bifurcation voltage, $\alpha u_i(X_1, X_2)$ is the perturbed displacement field, $\alpha\varphi(X_1, X_2)$ is the perturbed electric potential field, and α is a small parameter. The homogeneous film strain satisfies the equation,

$$\frac{\epsilon}{2}\left(\frac{V_0}{h}\right)^2 + \lambda\varepsilon_0(1 + \varepsilon_0)^2 + \mu(1 + \varepsilon_0)^3 - \mu(1 + \varepsilon_0) = 0 \tag{6}$$

The equilibrium equations and Gauss' law are expanded to order α^1 and yield equations governing the perturbed fields,

$$\frac{V_0}{(1+\varepsilon_0)h}u_{2,11} + \frac{V_0}{(1+\varepsilon_0)^3h}u_{2,22} - \varphi_{,11} - \frac{1}{(1+\varepsilon_0)^2}\varphi_{,22} = 0 \tag{7}$$

$$\left[\lambda + \mu + \frac{\mu}{(1+\varepsilon_0)^2}\right]u_{2,22} + \mu u_{2,11} + \left[(1 + \varepsilon_0)\lambda + \frac{\mu}{1+\varepsilon_0}\right]u_{1,21} = 0 \tag{8}$$

$$[(1 + \varepsilon_0)^2\lambda + 2\mu]u_{1,11} + \mu u_{1,22} + \left[(1 + \varepsilon_0)\lambda + \frac{\mu}{1+\varepsilon_0}\right]u_{2,21} = 0 \tag{9}$$

These equations are also subject to the voltage and traction-free boundary conditions on the surface of the film,

$$\varphi(X_1, 0) = 0 \tag{10}$$

$$\frac{\epsilon V_0}{h(1+\varepsilon_0)}\varphi_{,1}(X_1, 0) + \left[\frac{\mu}{1+\varepsilon_0} - \lambda\varepsilon_0 - \frac{\epsilon V_0^2}{2h(1+\varepsilon_0)^2}\right]u_{2,1}(X_1, 0) + \mu u_{1,2}(X_1, 0) = 0 \tag{11}$$

$$\frac{\epsilon V_0}{h(1+\varepsilon_0)^2}\varphi_{,3}(X_1, 0) + \left[\lambda + \frac{\mu}{1+\varepsilon_0} + \frac{\mu\varepsilon_0^2}{(1+\varepsilon_0)^2} - \frac{\epsilon V_0^2}{h(1+\varepsilon_0)^3}\right]u_{2,2}(X_1, 0) + \lambda(2 + \varepsilon_0)u_{1,1}(X_1, 0) = 0$$
$$\tag{12}$$

Taking the wavenumber of the wrinkling oscillations to be unity, and the wavelength of the oscillations to be much smaller than h, the solution to these equations is,

$$\varphi(X_1, X_2) = \frac{V_0}{h(1+\varepsilon_0)}\{u_2(X_1, X_2) - U_2(1 - A)\exp[(1 + \varepsilon_0)X_2]\cos(X_1)\} \tag{13}$$

$$u_2(X_1, X_2) = U_2\{\exp[X_2] - A\exp[pX_2]\}\cos(X_1) \tag{14}$$

$$u_1(X_1, X_2) = -U_2\left\{\frac{1}{1+\varepsilon_0}\exp[X_2] - \frac{A(1+\varepsilon_0)}{p}\exp[pX_2]\right\}\sin(X_1) \tag{15}$$

$$p = (1 + \varepsilon_0)\sqrt{\frac{2\mu+\lambda(1+\varepsilon_0)^2}{\mu+(\lambda+\mu)(1+\varepsilon_0)^2}} \tag{16}$$

$$A = \frac{\epsilon\left(\frac{V_0}{h}\right)^2 + 2(1+\varepsilon_0)[\varepsilon_0(1+\varepsilon_0)\lambda - 2\mu]}{\epsilon\left(\frac{V_0}{h}\right)^2 + 2(1+\varepsilon_0)[\varepsilon_0(\lambda-2\mu)+\varepsilon_0^2(\lambda-\mu)-2\mu]} \tag{17}$$

The critical value for V_0/h and the associated value for A result from an eigenvalue problem required to satisfy the boundary conditions with a non-trivial solution.

$$\frac{V_0}{h} = \sqrt{\frac{-b-\sqrt{b^2-4ac}}{2a}} \tag{18}$$

$$a = \frac{\epsilon^2[(1+\varepsilon_0)^2-p]}{4(1+\varepsilon_0)^2} \tag{19}$$

$$b = \frac{\epsilon[(1+\varepsilon_0)^2[\varepsilon_0(1+\varepsilon_0)\lambda-2\mu]-p\varepsilon_0(1+\varepsilon_0)\lambda+p(2+4\varepsilon_0+4\varepsilon_0^2+\varepsilon_0^3)\mu]}{1+\varepsilon_0} \tag{20}$$

$$c = (1 + \varepsilon_0)^2[\varepsilon_0(1 + \varepsilon_0)\lambda - 2\mu]^2 - p[\varepsilon_0(1 + \varepsilon_0)\lambda - (2 + 2\varepsilon_0 + \varepsilon_0^2)\mu]^2 \tag{21}$$

Equation (18) provides V_0/h in terms of ε_0, which then casts (6) as a single nonlinear algebraic equation governing ε_0. In the limit of incompressible behavior $\lambda \to \infty$, $\varepsilon_0 \to 0$, $p \to 1$, $a \to 0$, $b \to 2\epsilon\mu$, $c \to -4\mu^2$, and the solution for V_0/h becomes,

$$\frac{V_0}{h} = \sqrt{\frac{-c}{b}} = \sqrt{\frac{2\mu}{\epsilon}} \quad \text{as } \lambda \to \infty \tag{22}$$

The plot of $\sqrt{\epsilon/\mu}\,V_0/h$ as a function of λ/μ is given in Fig. 1b showing the approach to the limit $\sqrt{2}$. A second curve (dashed) has been included in Fig. 1b for another nonlinear isotropic elastic material whose incompressible limit is also the neo-Hookean material. Although the dependence on compressibility is different, the second model has the same limiting critical voltage as the first model. The free energy for the layer of second material is shown in the figure where $\kappa = \lambda + 2\mu/3$ is the bulk modulus.

In terms of the eigenvalue parameter introduced earlier, the incompressible limit is simply $\Omega = 2$ or $\sqrt{\varepsilon/\mu}\,V_0/h = \sqrt{2}$. The incorrect result obtained in the original paper is $\sqrt{\varepsilon/\mu}\,V_0/h = 1.287$. The correct result was first obtained by Huang (2005) who modeled the layer as an isotropic linearly elastic compressible material and took the result to the incompressible limit. Our subsequent work analyzing the non-objective linear elastic model of the layer within the finite strain context leads to the same incorrect result $\sqrt{\varepsilon/\mu}\,V_0/h = 1.287$ as in Hutchinson (2021). The inconsistency of the results for the linear elastic layer almost certainly stems from the fact that the linear elastic model is not objective in the finite strain context, whereas the two models used to generate the results in Fig. 1b are objective.

$$W = \frac{\mu}{2}\left(J^{-2/3}F_{ij}F_{ij} - 3\right) + \frac{\kappa}{4}\left(J^2 - 1 - \ln J^2\right) - \frac{\epsilon}{2}JF_{Ik}^{-1}F_{Jk}^{-1}E_I E_J$$

$$W = \frac{\mu}{2}\left(F_{ij}F_{ij} - 3\right) - \mu\ln J + \frac{\lambda}{2}\left(J - 1\right)^2 - \frac{\epsilon}{2}JF_{Ik}^{-1}F_{Jk}^{-1}E_I E_J$$
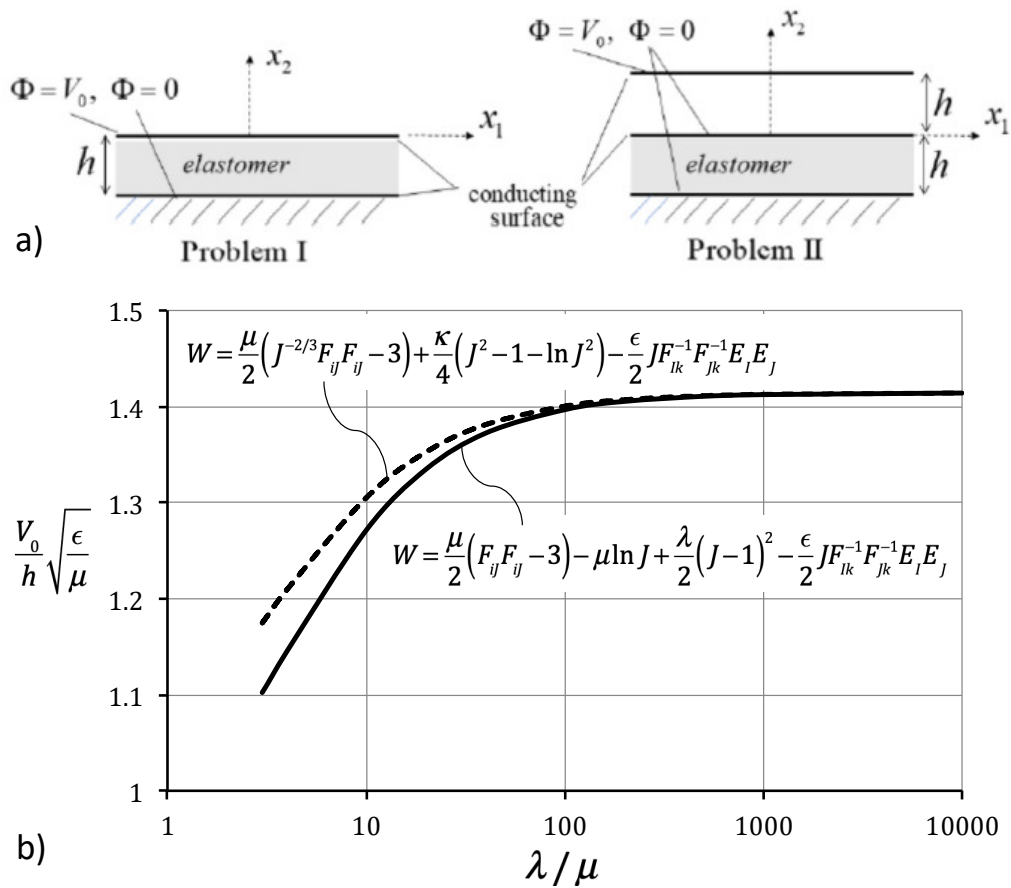
Fig. 1 a) Problems I and II. b) The dependence of the critical dimensionless voltage on the ratio of the two Lamé parameters showing the limit for Problem I as the material becomes incompressible for the material model discussed in the text (solid line) and for a second isotropic material model (dashed line and $\kappa = \lambda + 2\mu/3$) which also approaches the neo-Hookean model in the incompressible limit.

Results for the incompressible neo-Hookean layer from the corrected bifurcation functional (1) accounting for interaction with the bottom of the layer are presented in Fig. 2a for the case of no pre-stretch and several levels of surface energy measured by $\gamma / \mu h$. The lowest curve for a layer with no surface energy shows that the dimensionless critical voltage attains the short wavelength limit, $\sqrt{\Omega} = \sqrt{2}$, for all wavelengths satisfying $\ell / h < 1$. This plot also reveals the strong effect of the surface energy on the critical voltage at short wavelengths. Fig. 2b presents curves of the dimensionless critical voltage as a function of pre-stretch in the short wavelength limit for several values of the dimensionless surface energy, now as $\gamma / \mu \ell$, including the limit with $\gamma = 0$. An exact relatively simple analytical formula can be obtained for the short wavelength limit:

$$\Omega - \frac{2\pi\gamma}{\mu\ell} = \frac{\lambda_0^{9} + \lambda_0^{6} + 3\lambda_0^{3} - 1}{\lambda_0^{4}(\lambda_0^{3} + 1)} \tag{23}$$
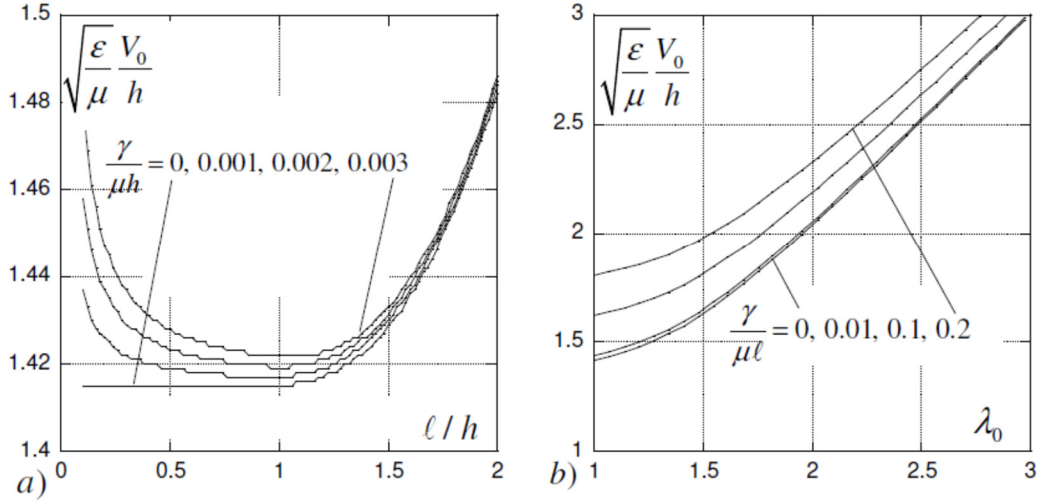

Fig. 2 Dimensionless voltage at bifurcation as dependent on wavelength, surface energy and pre-stretch for the incompressible neo-Hookean layer. a) As dependent on wavelength and surface energy with no pre-stretch. b) As dependent on pre-stretch and surface energy in the short wavelength limit when $\ell / h < 1$.

Stiffening greater than that predicted by the neo-Hookean material is commonly observed for some elastomers, which is expected to impact the effect of pre-stretch. The Gent generalization of the neo-Hookean material captures stiffening with a single additional parameter J_L, c.f., discussion in Section 6 and eq. (6.1) of the original paper. Fig. 3 displays the effect of the Gent parameter on the critical dimensionless voltage as dependent on pre-stretch in the short wavelength limit ($\ell / h < 1$) for layers with no surface energy computed using the corrected functional (1). The results in Fig. 2 and 3 apply to both Problems I & II.

The corrected bifurcation results for the critical voltage for the pre-stretched neo-Hookean material in Problem I are in much better agreement with the creasing experiments of Wang et al. (2011) than the previous erroneous ones. At a pre-stretch $\lambda_0 = 3$, the experimental critical voltages have a scatter of about 15% with the corrected bifurcation voltage falling in the center of the scatter. Because creasing is an unstable phenomenon and sensitive to small imperfections, one would expect the experimental data to consistently fall somewhat below the bifurcation prediction. This suggests that some stiffening effect such as that captured by the Gent model may be at play at the larger pre-stretches. In addition, the inconsistency noted in Section 6 of Hutchinson (2021) concerning the existing numerical prediction of the crease threshold for pre-stretched neo-Hookean materials still stands because that prediction falls above the corrected bifurcation result when $\lambda_0 \geq 2$.
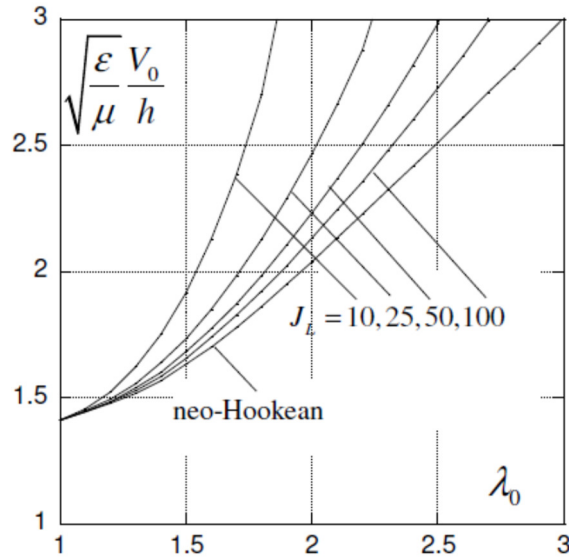

Fig. 3 The influence of the Gent stiffening parameter, J_L, on the critical dimensionless voltage as a function of pre-stretch in the short wavelength limit in the absence of surface energy.

The error in the bifurcation analysis carries into the post-bifurcation analysis and has a effect on the role of pre-stretch. The revision of the post-bifurcation analysis is presented in the Supplementary Materials attached to the errata. Here, we include Fig. 4 for Problem I which reveals that pre-stretch tends to reduce the level of instability at bifurcation. Let V_0^C be the voltage at bifurcation and V_0 be the voltage in the initial post-bifurcation regime. The initial post-bifurcation analysis determines the nonlinear coupling of the shortwave length modes and generates the lowest order dependence of quantities of interest on the eigenmodal mode amplitudes. Fig. 4a plots the lowest order asymptotic dependence of V_0 / V_0^C on the maximum

downward deflection of the layer normalized by ℓ, $-u_2(0,0)/\ell$, for seven values of the pre-stretch ranging from no pre-stretch to $\lambda_0 = 2.5$. In the uniform state the capacitance of a section of the layer of thickness h, length ℓ and unit depth is $C_0 = \varepsilon \ell / h$. The increased capacitance of this section in the bifurcation state is plotted in Fig. 4b for the same values of pre-stretch. The primary insight into the effect of pre-stretch on the level of instability is given by Fig. 4c where the voltage is plotted against the electrical charge in the section, c. For the uniform layer, $c = C_0 V_0$, and the value at bifurcation is $c_C = C_0 V_0^C$. With no pre-stretch, or relatively small pre-stretch, bifurcation is highly unstable under either prescribed voltage or charge. For increased levels pre-stretch above about $\lambda_0 = 2$ the initial post-bifurcation response falls less dramatically.

It must be emphasized that these results are the result of an asymptotic analysis perturbing about the bifurcation point, and their range of applicability into the post-bifurcation regime is unknown. The corresponding results for Problem II are presented in the revised Supplementary Materials. A detailed numerical analysis of the post-bifurcation behavior is underway which is not subject to the limitations of the current asymptotic perturbation analysis.
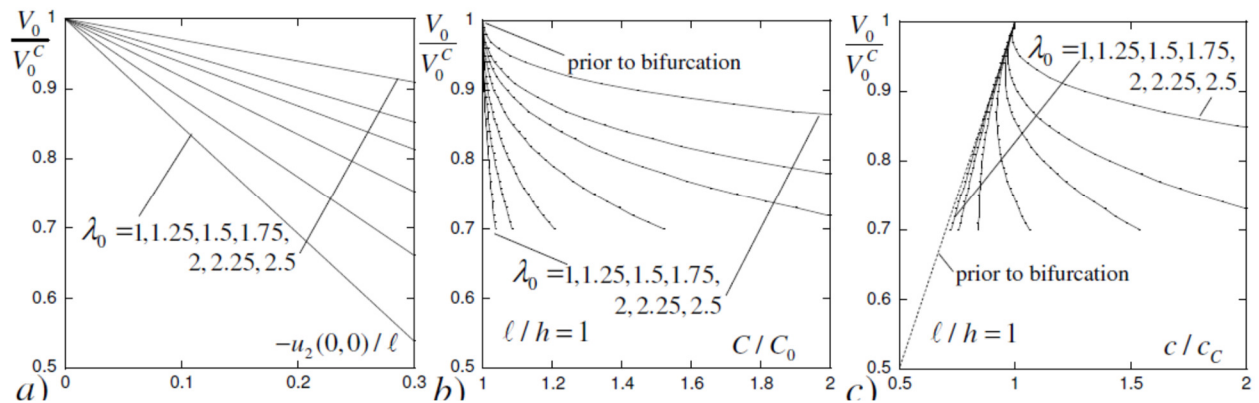

Fig. 4 The influence of pre-stretch, λ_0, on the initial post-bifurcation behavior of the constrained incompressible layer for Problem I. a) Voltage versus amplitude of the surface bifurcation deflection. b) Ratio of the capacitance in the initial post-bifurcation regime to the capacitance of the uniform layer. c) Voltage versus electrical charge in the initial post-bifurcation regime. These plots were computed using 6 modes; plots b) and c) were computed with $\ell / h = 1$.

References:

Boyce, M/C., and Arruda, E. M., 2000. Constitutive models for rubber elasticity: a review. Rubber Chemistry and Technology 73, 504-523.

Huang, R., 2005. Electrically induced surface instability of a conductive thin film on a dielectric substrate. Applied Physics Letters 87, 151911.

Hutchinson, J. W., 2021. Surface instabilities of constrained elastomeric layers subject to electro-static stressing. J. Mech. Phys. Solids 153, 104462.

Wang, Q., Tahir, M., Zhang, L., Zhao, X., 2011. Electro-creasing instability in deformed polymers: experiments and theory, Soft Mater. 7, 6583-6589.

Supporting Materials

Errata: Surface instabilities of constrained elastomeric layers subject to electro-static stressing

John W. Hutchinson

School of Engineering and Applied Sciences,

Harvard University, Cambridge, MA, 02138

These Supporting Materials include corrections to the original paper (Hutchinson, 2021) which did not appear in the Errata and changes in the original Supporting Materials which follow from the error in the bifurcation analysis, and which also did not appear in the brief Errata. The equation and figure numbers in the Errata Supporting Materials will be prefaced by the initials, ESM, numbers in the original Supporting Materials by the initials, SM, in the Errata itself by the initial, E. The equations and figures in the original paper (Hutchinson, 2021) are listed without any initial designation. The references cited in this document are those listed at the end of the original paper with a few additional references provided at the end of this document. We begin by filling in some details of the bifurcation analysis of the finite thickness layers, including discussion of the short wavelength limit, anticipating results from the second part of this document on development of the free energy functional and the post-bifurcation analysis for the short wavelength limit.

Bifurcation (linear stability) analysis including pre-stretch and surface energy

We begin with the quadratic plane strain bifurcation functional written for the finite thickness neo-Hookean layer with pre-stretch λ_0. Here, the dimensionless coordinates are $(x, y) = (kx_1, kx_2)$, and the dimensionless displacements are taken to be the dimensional ones divided by $\ell = 2\pi / k$, i.e., $(u_1 / \ell, u_2 / \ell)$ becoming (u_1, u_2). Recall that the horizontal and vertical displacements of a material point at (x_1, x_2) in the pre-stretched, pre-bifurcation, state, $(u_1(x_1, x_2), u_2(x_1, x_2))$, are employed. The corrected dimensionless quadratic bifurcation function for Problems I and II for one periodic section per unit depth in the x_3 direction is

$$\frac{\Delta\Psi_2}{\mu\ell^2} = \int_{-y_B}^{0}\int_{-\pi}^{\pi}\left\{\tfrac{1}{2}\lambda_0^{\ 2}\left(u_{1,x}^{\ 2} + u_{2,x}^{\ 2}\right) + \tfrac{1}{2}\lambda_0^{\ -4}\left(u_{1,y}^{\ 2} + u_{2,y}^{\ 2}\right)\right.$$

$$-\lambda_0^{\ -4}\left(u_{1,x}u_{2,y} - u_{1,y}u_{2,x}\right) - \Delta q(u_{1,x} + u_{2,y})/2\pi\Big\}\,dxdy \qquad\text{(ESM-1)}$$

$$+\pi\frac{\gamma}{\mu\ell}\int_{-\pi}^{\pi} u_2(x,0)_{,x}^{\ 2}\,dx - \frac{\pi}{2}\Omega\sum_{j=1}^{\infty}\text{cotanh}(jy_B)\,j\,v_j^{\ 2}$$

with $y_B = 2\pi h/\ell$ and $v_j = \pi^{-1}\int_{-\pi}^{\pi} u_2(x,0)\cos(jx)dx$. The last contribution from the electro-

static forces will be derived below. The first order incompressibility condition is enforced with

the Lagrangian multiplier, Δq, which is dimensionless with period ℓ.

One can proceed in several ways. The procedure used here is as follows. In the first

step, generate the linear system of pde's and boundary conditions that render $\Delta\Psi_2$ stationary

subject to $u_1(x,-y_B) = u_2(x,-y_B) = 0$. The details of this step are omitted here but we use the

fact that these pde's, boundary conditions and the periodicity requirement admit separated

solutions of the form

$$u_1 = U(y)\sin x,\ u_2 = V(y)\cos x,\ \Delta q = Q(y)\cos x \qquad\text{(ESM-2)}$$

Substitution of these back into (ESM-1) and integrating with respect to x gives

$$\frac{\Delta\Psi_2}{\mu\ell^2} = \pi\int_{-y_B}^{0}\left\{\tfrac{1}{2}\lambda_0^{\ 2}\left(U^2 + V^2\right) + \tfrac{1}{2}\lambda_0^{\ -4}\left(U'^2 + V'^2\right) - \lambda_0^{\ -4}\left(UV' + U'V\right) - \tfrac{1}{2\pi}Q(U + V')\right\}dy - \frac{\pi}{2}\Gamma V(0)^2 \ \text{(ESM-3)}$$

with $\Gamma = \Omega\text{cotanh}(y_B) - 2\pi\gamma h/(\mu\ell)$ and $(\ )' = d(\ )/dy$. Rendering $\Delta\Psi_2$ stationary with

respect to U, V and Q subject to $U(-y_B) = 0$ and $V(-y_B) = 0$ requires

$$\left.\begin{aligned} \lambda_0^{\ -4}U'' - \lambda_0^{\ 2}U + Q/2\pi &= 0\\ \lambda_0^{\ -4}V'' - \lambda_0^{\ 2}V - Q'/2\pi &= 0\\ U + V' &= 0 \end{aligned}\right\}\ \text{for}\ -y_B \le y \le 0 \qquad\text{(ESM-4)}$$

together with the boundary conditions

$$\lambda_0^{-4}U' - \lambda_0^{-4}V = 0 \quad (y=0)$$
$$2\lambda_0^{-4}V' - 2\lambda_0^{-4}U - Q/2\pi - \Gamma\mathrm{cotanh}(y_B)V = 0 \quad (y=0)$$
$$U = 0 \quad (y=-y_B)$$
$$V = 0 \quad (y=-y_B)$$

(ESM-5)

If $\lambda_0 = 1$, the linearly independent solutions to the 4th order system (ESM-4) are

$$U = -c_1 e^y - c_2(1+y)e^y + c_3 e^{-y} - c_4(1-y)e^{-y}$$
$$V = c_1 e^y + c_2 y e^y + c_3 e^{-y} + c_4 y e^{-y}$$
$$Q = 2\pi\left(2c_2 e^y + 2c_4 e^{-y}\right)$$

(ESM-6)

If $\lambda_0 > 1$, the solutions are

$$U = -c_1 e^y - c_2\lambda_0^3 e^{\lambda_0^3 y} + c_3 e^{-y} + c_4\lambda_0^3 e^{-\lambda_0^3 y}$$
$$V = c_1 e^y + c_2 e^{\lambda_0^3 y} + c_3 e^{-y} + c_4 e^{-\lambda_0^3 y}$$
$$Q = 2\pi(\lambda_0^2 - \lambda_0^{-4})\left(-c_1 e^y + c_3 e^{-y}\right)$$

(ESM-7)

Two methods to generate solutions to the eigenvalue problem for the finite thickness layer are outlined below. For each method, first express c_3 and c_4 in terms of c_1 and c_2 by enforcing the boundary conditions on $y = -y_B$ in (ESM-5). Then, express the two boundary conditions on $y = 0$ in (ESM-5) which provides 2 linear homogeneous equations for c_1 and c_2. The requirement that the determinant of this system vanish is the desired condition for the eigenvalues Ω or, equivalently, Γ. In addition to the pre-stretch, λ_0, and dimensionless surface energy, $\gamma/\mu\ell = (\gamma/\mu h)(h/\ell)$, the only parameter is the dimensionless layer thickness $y_B = 2\pi h/\ell$. The critical (lowest) eigenvalue is minimized with respect to the dimensionless mode number $h/\ell = hk/2\pi$, which as seen in the Fig E2a occurs as the short wavelength limit when the surface energy is zero. Alternatively, one can evaluate $\Delta\Psi_2/\mu\ell^2$ in (ESM-3) in terms of c_1 and c_2 using numerical integration for any specified set of parameters and then evaluate Ω or Γ from the boundary conditions on the top surface. Considering all possible mode numbers, the critical eigenvalue is the lowest value of Ω for which $\Delta\Psi_2/\mu\ell^2 = 0$. These two

methods are readily implemented and yield results of high accuracy using standard numerical algorithms with double precision arithmetic.

It is difficult to produce uncomplicated closed form formulas by carrying out either of the above procedures analytically when the critical mode interacts with the bottom of the layer. However, when the critical eigenvalue lies within the short wavelength limit, an exact and simple analytical formula for the lowest eigenvalue and associated eigenmodes can be obtained. In the short wavelength limit $y_B = 2\pi h / \ell \to \infty$ in (ESM-3) - (ESM-5) with $c_3 = c_4 = 0$ and $\coth(y_B) = 1$. The boundary conditions on $y = 0$ in (ESM-5) provide the eigenvalue condition. These can be reduced analytically to the give the formula for the critical eigenvalue, (ESM-23). The associated eigenmodes normalized such that $V(0) = 1$ are

$$U = y e^y, \ V = e^y - y e^y, \ Q / 2\pi = -2 e^y \ \text{for} \ \lambda_0 = 1$$

$$U = \frac{1}{p^2 - 1}\left(-(p^2 + 1)e^y + 2 p e^{py}\right), \ V = \frac{1}{p^2 - 1}\left((p^2 + 1)e^y - 2 e^{py}\right),$$

$$\frac{Q}{2\pi} = -\frac{p^2 + 1}{p \lambda_0}e^y$$

for $\lambda_0 > 1$ with $p = \lambda_0^3$.

In carrying out the bifurcation analysis for other constitutive models, such as the Gent model, using the methods employed in this paper, one must derive the quadratic bifurcation functional for the specific model. We have used both a direct approach and Hill's (1961) alternative approach to bifurcation in finitely strained solid bodies, which is similar in some respects to that of Biot (1965). These approaches lead to the following quadratic bifurcation functional for the Gent material:

$$\frac{\Delta\Psi_2}{\mu\ell^2} = \int_{-y_B}^{0} dy \int_{-\pi}^{\pi} dx \left\{ \frac{1}{2\omega_0}\left[\lambda_0^2\left(u_{1,x}^2 + u_{2,x}^2\right) + \lambda_0^{-4}\left(u_{1,y}^2 + u_{2,y}^2\right) + \frac{2}{\omega_0 J_L}\left(\lambda_0^2 u_{1,x} + \lambda_0^{-4}u_{2,y}\right)^2 \right. \right.$$
$$\left. -2\lambda_0^{-4}\left(u_{1,x}u_{2,y} - u_{1,y}u_{2,x}\right)\right] - \frac{\Delta q}{2\pi}\left(u_{1,x} + u_{2,y}\right)\right\} + \pi\frac{\gamma}{\mu\ell}\int_{-\pi}^{\pi} u_2(x,0)_{,x}^2 dx - \frac{\pi}{2}\Omega\sum_{j=1}^{\infty}\coth(jy_B)j v_j^2$$

Here, $\omega_0 = 1 - (2\lambda_0^2 + \lambda_0^{-2} - 3)/J_L$ and J_L is the Gent stiffening parameter with the full energy density defined in (6.1). In the limit $J_L \to \infty$ for the neo-Hookean material (c.f., ESM-1) the quadratic terms for the elastic energy constitute the entire elastic energy subject to the full exact incompressibility constraint: $u_{1,x} + u_{2,y} + u_{1,x}u_{2,y} - u_{1,y}u_{2,x} = 0$. Terms in the elastic energy smaller than quadratic have been neglected for the Gent material.

The electro-static energy changes for deformations of period ℓ

In this section, we fill in some of the omitted steps, simplifying and correcting the presentation of Section 3.2 and the Supplementary Materials in the original paper. First consider Problem I. Application of Green's theorem to (3.6), transforms it to an integral along the boundary C,

$$
\begin{aligned}
\Delta U_{electric} &= \frac{1}{2}\varepsilon V_0'^2 \int_{-\ell/2}^{\ell/2} \left(2\varphi + \varphi\varphi_{,i}n_i\sqrt{1+Y'^2} \right) dx_1 \\
&= \frac{1}{2}\varepsilon V_0'^2 \int_{-\ell/2}^{\ell/2} \varphi\varphi_{,i}n_i\sqrt{1+Y'^2}\,dx_1 = \frac{1}{2}\varepsilon V_0'^2 \int_{-\ell/2}^{\ell/2} Y\left(Y'\varphi_{,1} - \varphi_{,2}\right)dx_1
\end{aligned}
$$
(ESM-8)

Here, n_i is the unit normal to C with components $n_1 = -Y'/\sqrt{1+Y'^2}$ and $n_2 = 1/\sqrt{1+Y'^2}$ where $Y' = dY/dx_1$ (see Fig. 6 for Problem I). In applying Green's theorem, the contributions from the vertical sides of the section in Fig. 3 cancel each other by periodicity and the contribution along the bottom of the layer vanishes because $\varphi = 0$. Because $\varphi = -Y$ on C,

$$
\int_{-\ell/2}^{\ell/2} \varphi\,dx_1 = -\int_{-\ell/2}^{\ell/2} Y(x_1)\,dx_1 = 0 .
$$

The next step is to solve for the change in the potential φ as dependent on the shape change Y and to evaluate (ESM-8). The stability analysis conducted in this paper requires $\Delta U_{electric}$ to be known to order Y^3, and we will neglect contributions of order Y^4 and smaller.

Using a Fourier series, $\varphi(x_1, x_2) = \sum_{j=0}^{\infty} f_j(x_2)\cos(jkx_1)$, with $k = 2\pi/\ell$ (consistent with symmetry about $x_1 = 0$), one finds the solution to $\nabla^2\varphi = 0$ with $\varphi = -Y$ on C to be

$$\varphi(x_1, x_2) = \varphi_0(x_2/h + 1) + \sum_{j=1}^{\infty} \varphi_j e^{jkx_2} \cos(jkx_1) \qquad \text{(ESM-10)}$$

with the coefficients φ_j required to satisfy

$$\varphi_0\left(Y(x_1)/h + 1\right) + \sum_{j=1}^{\infty} \varphi_j e^{jkY(x_1)} \cos(jkx_1) = -Y(x_1) \qquad \text{(ESM-11)}$$

(The solution above must be modified when the wavelength is not sufficiently short to satisfy the condition $\varphi = 0$ on $x_2 = -h$. From this point on, we limit attention to the short wavelength limit for which ℓ/h is sufficiently small such that terms like $e^{-2\pi h/\ell}$ can be neglected, i.e., the undulations of the surface do not interact with the bottom of the layer. To obtain the electro-static term, $\Omega \coth(y_B)V(0)^2$, in the bifurcation functional (E-1) when the wavelength is not short, one proceeds by producing the solution above that satisfies $\varphi = 0$ at the bottom of the layer. This extension is straightforward for the bifurcation problem because the Fourier coefficients are only needed to order Y.)

The solution for the Fourier coefficients from (ESM-10b) to order Y^2, required to obtain $\Delta U_{electric}$ to order Y^3, is

$$\varphi_0 = \frac{k}{2}\sum_{j=1}^{\infty} jY_j^2$$

$$\varphi_j = -Y_j + \frac{k}{\pi}\sum_{m=1}^{\infty}\sum_{i=1}^{\infty} mA_{jmi}Y_mY_i, \qquad j \geq 1 \qquad \text{(ESM-12)}$$

where $Y_j = (2/\ell)\int_{-\ell/2}^{\ell/2} Y(x_))dx_1$ and

$$A_{jmi} = \int_{-\pi}^{\pi} \cos jx \cos mx \cos ix\, dx$$

$$= \frac{\pi}{2}\left(\alpha(j+m+i) + \alpha(-j+m+i) + \alpha(j-m+i) + \alpha(j+m-i)\right)$$

with $\alpha(j) = 1$ if $j = 0$ and $\alpha(j) = 0$ if $j \neq 0$. Note that $A_{jmi} = A_{mji} = A_{imj}$.

The results needed to evaluate $\Delta U_{electric}$ in (ESM-8) to order Y^3 have been obtained. The result is

$$\Delta U_{electrix} = \frac{1}{2}\varepsilon\left(\frac{V_0}{h}\right)^2 \left\{\pi\sum_{j=1}^{\infty} jY_j^2 + k\sum_{j=1}^{\infty}\sum_{m=1}^{\infty}\sum_{i=1}^{\infty}\left(j(j-m)A_{jmi} - miB_{jmi}\right)Y_jY_mY_i\right\} \quad (\text{ESM-13})$$

where

$$B_{jmi} = \int_{-\pi}^{\pi} \cos jx \sin mx \sin ix\, dx$$

$$= \frac{\pi}{2}\left(\alpha(j+m-i) + \alpha(j-m+i) - \alpha(j+m+i) - \alpha(-j+m+i)\right)$$

In general, $B_{jni} \neq B_{mji}$, but $B_{jmi} = B_{jim}$.

As noted in Section (3.3) of the original paper, the last step is transforming (ESM-13) into the surface shape expressed in terms of the displacement components of the surface, $u_i(x_1,0)$, whose Fourier series are $u_1 = \sum_{j=1}^{\infty}(u_1)_j \sin jkx_1$ and $u_2 = \sum_{j=1}^{\infty}(u_2)_j \cos jkx_1$ with

$$(u_1)_j = (2/\ell)\int_{-\ell/2}^{\ell/2} u_1(x_1,0)\sin(jkx_1)dx_1 \quad \text{and} \quad (u_2)_j = (2/\ell)\int_{-\ell/2}^{\ell/2} u_2(x_1,0)\cos(jkx_1)dx_1$$

To the order of accuracy required in this investigation, the relation $Y(x_1) = u_2(\overline{x}_1,0)$ with $x_1 = \overline{x}_1 + u_1(\overline{x}_1,0)$ can be replaced by $Y(x_1) = u_2(x_1,0) - u_1(x_1,0)\,du_2(x_1,0)/dx_1$, which, in turn, provides

$$Y_j = (u_2)_j + \frac{k}{\pi}\sum_{m=1}^{\infty}\sum_{i=1}^{\infty} iB_{jmi}(u_1)_m(u_2)_i = (u_2)_j - \frac{k}{\pi}\sum_{m=1}^{\infty}\sum_{i=1}^{\infty} iB_{jmi}\frac{p-1}{p+1}(u_2)_m(u_2)_i$$

where the connection $(u_1)_j = -[(p-1)/(p+1)](u_2)_j$ with $p = \lambda_0^3$ (which will be derived later) has been to obtain the last expression. Applying this transformation to (ESM-13) and neglecting terms of order u^4, gives

$$\Delta U_{electrix} = \frac{1}{2}\varepsilon\left(\frac{V_0}{h}\right)^2 \left\{ \pi \sum_{j=1}^{\infty} j(u_2)_j^2 \right.$$

$$\left. +k\sum_{j=1}^{\infty}\sum_{m=1}^{\infty}\sum_{i=1}^{\infty}\left[\tau\left(j(j-m)A_{jmi} - miB_{jmi}\right) - 2[(p-1)/(p+1)]jiB_{jmi}\right](u_2)_j(u_2)_m(u_2)_i \right\}$$

(ESM-14)

The presence of the factor τ will be explained shortly; for Problem I, $\tau = 1$.

The full free energy functional for the system to order u^3 consisting of the contributions from the elastic deformation and the electro-static forces for prescribed voltage V_0 can now be presented. We do so below in dimensionless form with the displacement components normalized by the wavelength ℓ but still expressed as u_i, Δq is dimensionless and is unchanged, and the dimensionless coordinates are $(x, y) = k(x_1, x_2)$ such that $-\pi \le x \le \pi$. Recall that $\Omega = (\varepsilon / \mu)(V_0 / h)^2$. The functional for the neo-Hookean material with equi-biaxial pre-stretch λ_0 and no surface energy is

$$\frac{\Delta\Psi}{\mu\ell^2} = \int_{-\infty}^{0}\int_{-\pi}^{\pi}\left\{\frac{1}{2}\lambda_0^2\left(u_{1,x}^2 + u_{2,x}^2\right) + \frac{1}{2}\lambda_0^{-4}\left(u_{1,y}^2 + u_{2,y}^2\right)\right.$$

$$\left. -(\lambda_0^{-4} + \Delta q)\left(u_{1,x}u_{2,y} - u_{1,y}u_{2,x}\right) - \Delta q(u_{1,x} + u_{2,y})/2\pi\right\}dxdy$$

$$-\frac{\pi}{2}\Omega\left\{\sum_{j=1}^{\infty} j(u_2)_j^2\right.$$

(ESM-15)

$$\left. +2\sum_{j=1}^{\infty}\sum_{m=1}^{\infty}\sum_{i=1}^{\infty}\left[\tau\left(j(j-m)A_{jmi} - miB_{jmi}\right) - 2[(p-1)/(p+1)]jiB_{jmi}\right](u_2)_j(u_2)_m(u_2)_i \right\}$$

where the Fourier coefficients of the dimensionless displacement components are

$$(u_1)_j = \pi^{-1}\int_{-\pi}^{\pi} u_1(x,0)\sin jx\, dx \quad \& \quad (u_2)_j = \pi^{-1}\int_{-\pi}^{\pi} u_2(x,0)\cos jx\, dx$$

If similar procedures are followed for Problem II accounting for the fact that C is the boundary at the bottom of the periodic sector between the two electrodes (see Fig. 6) and ε is the permittivity of the medium above the elastomer layer, one finds the same result as in (ESM-13) but with a sign change for the cubic terms. It is easy to see this result in another way by noting that the electro-static energy contribution for Problem II with $Y(x_1) \rightarrow -Y(x_1)$ is identical to that of Problem I, assuming ε is the same in both problems. On the other hand, the

transformation from Y to u_1 and u_2 is the same for Problem II as I. Thus, for Problem II the free energy functional is also (ESM-15), but with $\tau = -1$, and with ε as the permittivity of the medium above the elastomer layer.

As remarked earlier, the elastic energy contribution has not been approximated and the full incompressibility constraint is included enforced by the Lagrangian multiplier Δq. The contribution from the electro-static terms is accurate to order u^3. As already noted, to order u^2 there is no difference in the functionals for Problems I and II, and thus the critical bifurcation voltage, Ω_C given by (E-23), i.e.,

$$\Omega_C = \frac{p^3 + p^2 + 3p - 1}{p(p+1)\lambda_0}, \quad p = \lambda_0^{\ 3} \tag{ESM-16}$$

is the same for the two problems, as are the eigenmodes. Differences between the two problems emerge in the post-bifurcation range.

In the short wavelength limit we consider N eigenmodes having the same critical eigenvalue Ω_C which are given by (for the dimensionless quantities)

$$(u_1, u_2, \Delta q) = \sum_{j=1}^{N} \xi^{(j)} \left(U^{(j)}(y) \sin jx, V^{(j)}(y) \cos jx, Q^{(j)}(y) \cos jx \right) \tag{ESM-17}$$

where the modes are normalized by requiring $V^{(j)}(0) = 1$ and $\xi^{(j)}$ is the amplitude of the jth mode. For $\lambda_0 > 1$ and with $p = \lambda_0^{\ 3}$, we have from results given earlier that

$$U^{(j)} = \frac{1}{p^2 - 1}\left(-(p^2+1)e^{jy} + 2pe^{jpy}\right), \ V^{(j)} = \frac{1}{p^2 - 1}\left((p^2+1)e^{jy} - 2e^{jpy}\right), \frac{Q^{(j)}}{2\pi} = -\frac{p^2+1}{p\lambda_0}e^{jy}$$

It is useful to note that $(u_1)_j = \xi^{(j)}U^{(j)}(0)$, $(u_2)_j = \xi^{(j)}V^{(j)}(0) = \xi^{(j)}$ and the result used in the transformation, $(u_1)_j = -(p-1)/(p+1)(u_2)_j = -(p-1)/(p+1)\xi^{(j)}$.

The initial post-bifurcation expansion with small initial imperfections

As discussed in Section 4.2 of the original paper, the analysis addresses a system with N linearly independent modes all of which have the same critical eigenvalue, Ω_C. The abstract notation introduced in Section 4.2 is also used here and we pick up the development assuming (4.5) - (4.10) of the original paper and considering at first that no imperfections are present.

If one substitutes the expansion (4.5) into $\Delta\Psi$ in (4.6), making use of the various relations in (4.7) - (4.10), one obtains

$$\Delta\Psi = \left(\Omega_C - \Omega\right)\sum_{i=1}^{N}\xi^{(i)2}G_2(u^{(i)}) + F_3\left(\sum_{i=1}^{N}\xi^{(i)}u^{(i)}\right) - \Omega G_3\left(\sum_{i=1}^{N}\xi^{(i)}u^{(i)}\right)$$
$$+ 2\sum_{i=1}^{N}\xi^{(i)}\left(F_{11}(u^{(i)},\Delta u) - \Omega G_{11}(u^{(i)},\Delta u)\right) + F_2(\Delta u) - \Omega G_2(\Delta u) + ...$$

(ESM-18)

The first two term on the second line vanish by orthogonality, while the last two are of order ξ^4 and will be neglected. Rendering $\Delta\Psi$ stationary with respect to the mode amplitudes will generate set of equations relating Ω to the mode amplitudes ξ of the form $\Omega = \Omega_C + O(\xi)$. Thus, to evaluate $\Delta\Psi$ to order ξ^3, the term ΩG_3 in (ESM-18)) can be replaced by $\Omega_C G_3$. With this replacement and retaining all terms to order ξ^3, (ESM-18) can be rewritten as

$$\Delta\Psi = \left(\Omega_C - \Omega\right)\sum_{i=1}^{N}\xi^{(i)2}G_2(u^{(i)}) + F_3\left(\sum_{i=1}^{N}\xi^{(i)}u^{(i)}\right) - \Omega_C G_3\left(\sum_{i=1}^{N}\xi^{(i)}u^{(i)}\right)$$

(ESM-19)

This can also be written as

$$\Delta\Psi = \left(1 - \Omega/\Omega_C\right)\sum_{i=1}^{N}c_i\xi^{(i)2} + \sum_{j=1}^{N}\sum_{m=1}^{N}\sum_{n=1}^{N}c_{jmn}\xi^{(j)}\xi^{(m)}\xi^{(n)}$$

(ESM-20)

where $c_i = \Omega_C G_2(u^{(i)})$ and the coefficients in the cubic term can be evaluated in terms of the eigenmodes using the cubic contributions in (ESM-19) without the need for solving for higher order terms.

The specific calculations in this paper will be calculated using the set of the first six simultaneous eigenmodes. For $N = 6$, the non-zero terms in (ESM-20) can be expressed as (4.12) and repeated here including the lowest order contribution from the initial imperfection whose amplitude in the jth mode is denoted by $\overline{\xi}^{(j)}$ and which will be defined precisely later:

$$\frac{\Delta\Psi}{\pi\mu\ell^2\Omega_C/2} = \left(1 - \Omega/\Omega_C\right)\sum_{j=1}^{6}j\xi^{(j)2} + a_1\xi^{(1)2}\xi^{(2)} + a_2\xi^{(1)}\xi^{(2)}\xi^{(3)} + a_3\xi^{(1)}\xi^{(3)}\xi^{(4)} + a_4\xi^{(1)}\xi^{(4)}\xi^{(5)}$$
$$+ a_5\xi^{(j)}\xi^{(5)}\xi^{(6)} + a_6\xi^{(2)2}\xi^{(4)} + a_7\xi^{(2)}\xi^{(3)}\xi^{(5)} + a_8\xi^{(2)}\xi^{(4)}\xi^{(6)} + a_9\xi^{(3)2}\xi^{(6)} + \sum_{j=1}^{6}\overline{a}_j\overline{\xi}^{(j)}\xi^{(j)}$$

(ESM-21)

The coefficients a_j are plotted in Fig. ESM-1 as a function pre-stretch for the range $1 \le \lambda_0 \le 3$ for Problems I and II. The coefficients for the imperfection contributions $\bar{a}_j$ are defined later. The values for no-pre-stretch can be computed using the eigenmodes in (ESM-17) for the limit $\lambda_0 = 1$ or to four place accuracy using (ESM-17) with $\lambda_0 = 1.0001$. For constructing the figures presented below these coefficients have been generated for each value of pre-stretch required.
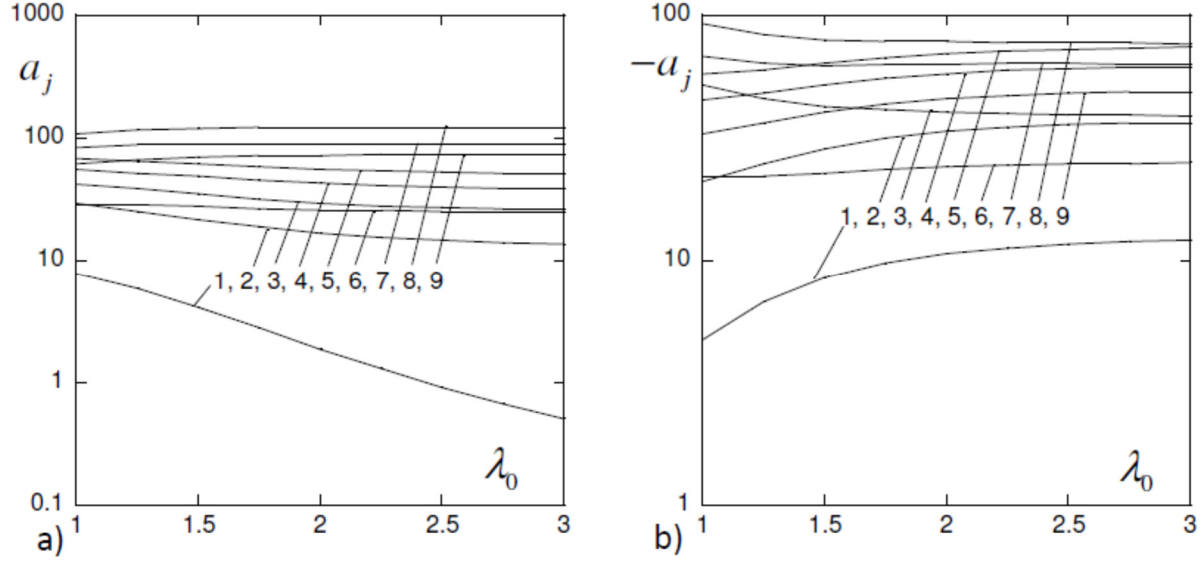

Fig. ESM-1. The cubic coefficients a_j for $j = 1,9$ ($N = 6$) as a function of pre-stretch for Problem I in a) and Problem II in b).

Stationarity of $\Delta\Psi$ in (ESM-21) with respect to each of the mode amplitudes generates the set of six simultaneous initial post-bifurcation equilibrium equations:

$$2\left(1-\Omega/\Omega_C\right)\xi^{(1)} + 2a_1\xi^{(1)}\xi^{(2)} + a_2\xi^{(2)}\xi^{3)} + a_3\xi^{(3)}\xi^{(4)} + a_4\xi^{(4)}\xi^{(5)} + a_5\xi^{(5)}\xi^{(6)} = -\bar{a}_1\bar{\xi}^{(1)}$$
$$4\left(1-\Omega/\Omega_C\right)\xi^{(2)} + a_1\xi^{(1)2} + a_2\xi^{(1)}\xi^{(3)} + 2a_6\xi^{(2)}\xi^{(4)} + a_7\xi^{(3)}\xi^{(5)} + a_8\xi^{(4)}\xi^{(6)} = -\bar{a}_2\bar{\xi}^{(2)}$$
$$6\left(1-\Omega/\Omega_C\right)\xi^{(3)} + ...$$
$$8 \quad ....$$

(ESM-22)

For the perfect system ($\bar{\xi}^{(j)} = 0$, $j = 1, N$), solutions have the form $\xi^{(j)} = (1-\Omega/\Omega_C)z_j$ where the six simultaneous equations for the constants, z_j, $j = 1,6$ are

$$2z_1 + 2a_1 z_1 z_2 + a_2 z_2 z_3 + a_3 z_3 z_4 + a_4 z_4 z_5 + a_5 z_5 z_6 = 0$$
$$4z_2 + a_1 z_1^2 + a_2 z_1 z_3 + 2a_6 z_2 z_4 + a_7 z_3 z_5 + a_8 z_4 z_6 = 0$$
$$6z_3 + ...$$
$$8 \ ....$$

(ESM-23)

Solutions to the six simultaneous algebraic equations (ESM-23) presented here using the ISML subroutine DNEQNF (Visual Numerics, 1994) with an initial guess that takes z_1 and z_2 as the only non-zero values with $z_1 = -2/a_1$ and $z_2 = -1/a_1$. The normal displacement to the surface in the initial post-bifurcation response is given by (in dimensional form)

$$u_2(x_1,0)/\ell = \left(!-\Omega/\Omega_C\right)\sum_{j=1}^{N} z_j \cos(jkx_1) \text{ with } u_2(0,0)/\ell = \left(!-\Omega/\Omega_C\right)\sum_{j=1}^{N} z_j \text{ (ESM-24)}$$

Plots of the maximum downward deflection of the layer surface, $-u_2(0,0)/\ell$, as dependent on Ω/Ω_C from this formula are for increasing levels of pre-stretch in Fig. E-4a.

The relation connecting the electrical charge, c, voltage, V_0, capacitance, C, and electrical energy, $U_{electrical}$, is

$$U_{electric} = \frac{1}{2}cV_0 = \frac{1}{2}CV_0^2$$

For Problem I, for a section of the dielectric elastomer of initial length ℓ, height h and unit depth, the electrical energy is given by

$$U_{electric} = \frac{1}{2}\varepsilon\left(\frac{V_0}{h}\right)^2 \ell h + \Delta U_{electric}$$

Evaluating $\Delta U_{electric}$ using (ESM-14) with $\xi^{(j)} = (1-\Omega/\Omega_C)z_j$ gives

$$\Delta U_{electric} = \frac{\pi}{2}\varepsilon\left(\frac{V_0}{h}\right)^2 \ell^2 \left\{\left(1-\frac{\Omega}{\Omega_C}\right)^2 s_2 + \left(1-\frac{\Omega}{\Omega_C}\right)^3 s_3\right\}$$

where $s_2 = \sum_{j=1}^{N} jz_j^2$ and

$$s_3 = 2\sum_{j=1}^{\infty}\sum_{m=1}^{\infty}\sum_{i=1}^{\infty}\left[\tau\left(j(j-m)A_{jmi} - miB_{jmi}\right) - 2[(p-1)/(p+1)]jiB_{jmi}\right]z_j z_m z_i\bigg\}$$

With $C_0 = \varepsilon\ell/h$ as the capacitance of the uniform section and $C = 2U_{electric}/V_0^2$ as the capacitance in the bifurcated state,

$$\frac{C}{C_0} = \left\{1 + \frac{\ell}{h}\pi\left(s_2(1-\Omega/\Omega_C)^2 + s_3(1-\Omega/\Omega_C)^3\right)\right\}$$
$$= \left\{1 + \frac{\ell}{h}\pi\left(2s_2(1-V_0/V_0^C)^2 + (-4s_2+8s_3)(1-V_0/V_0^C)^3\right)\right\}$$

(ESM-24)

accurate to order $(1-V_0/V_0^C)^3$. This relation is plotted for seven values of λ_0 in Fig. E4b for $\ell/h = 1$. Finally, with $c_C = C_0 V_0^C$ as the electric charge at bifurcation, the relation between the charge and the voltage in the initial post-bifurcation range, $c = CV_0$, is given by

$$\frac{c}{c_C} = \frac{C}{C_0}\frac{V_0}{V_0^C} = \left\{1 + \frac{\ell}{h}\pi\left(2s_2(1-V_0/V_0^C)^2 + (-4s_2+8s_3)(1-V_0/V_0^C)^3\right)\right\}\frac{V_0}{V_0^C}$$

(ESM-25)

This relation is plotted for the same seven values of pre-stretch in Fig. E4c. With no pre-stretch, or relatively small pre-stretch, bifurcation is highly unstable under either prescribed voltage or charge. For increased levels pre-stretch above about $\lambda_0 = 2$ the initial post-bifurcation response falls much less dramatically.

The results for Problem I presented above were computed using $\tau = 1$. For Problem II the formulas presented above apply with $\tau = -1$. Fig. ESM -2 below presents the corresponding results to those just discussed for Problem II. The two sets of results differ in two important respects. First, the maximum amplitude of the surface deflection is downward in Problem I while it is upward in Problem II, in each case the deformation acts to bring the two electrode surfaces closer together subject to the incompressibility constraint. The second important difference between the two problems is that pre-stretch over the range $1 \le \lambda_0 \le 2.5$ reduces the

severity of the instability in Problem I, while the severity of instability is somewhat increased for Problem II. The difference in the severity of the instability between the two problems is seen in the imperfection-sensitivity dependence on pre-stretch in Fig. ESM-3 for an perturbing force imperfection with amplitude $\overline{\xi}_1$ defined in the last sub-section just below. The maximum voltage, $(V_0)_{max}$, the system can sustain prior to instability normalized by the maximum for the perfect system (the bifurcation volage), V_0^C, is plotted as a function of pre-stretch for two imperfection levels. The role of pre-stretch on the layer nonlinearity in enhancing the instability of upward ridge-like modes and suppressing the instability of downward crease-like modes has been discussed by Zang et al. (2012) and Hutchinson (2013).
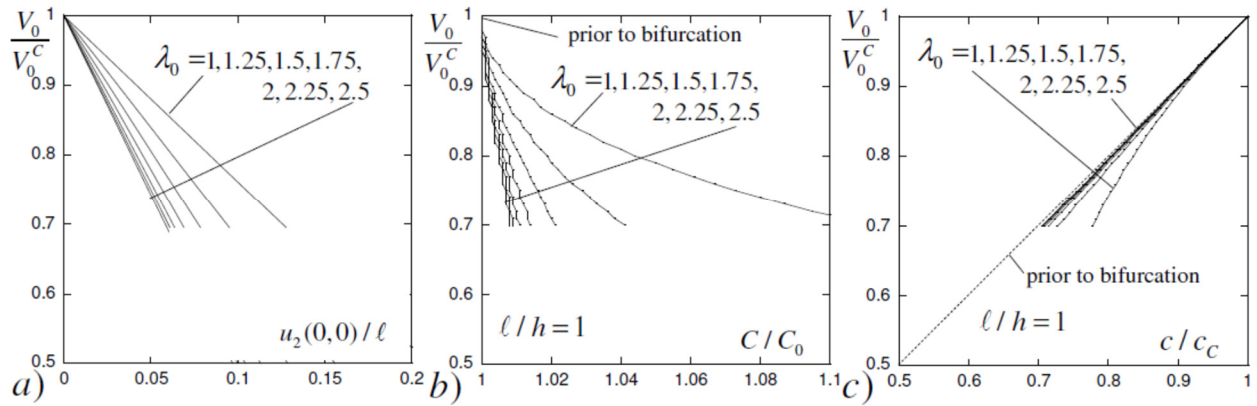

Fig. ESM-2 The influence of pre-stretch, λ_0, on the initial post-bifurcation behavior of the constrained incompressible layer for Problem II. a) Voltage versus amplitude of the surface bifurcation deflection. b) Ratio of the capacitance in the initial post-bifurcation regime to the capacitance of the uniform layer. c) Voltage versus electrical charge in the initial post-bifurcation regime. These plots were computed using 6 modes; plots b) and c) were computed with $\ell/h = 1$.
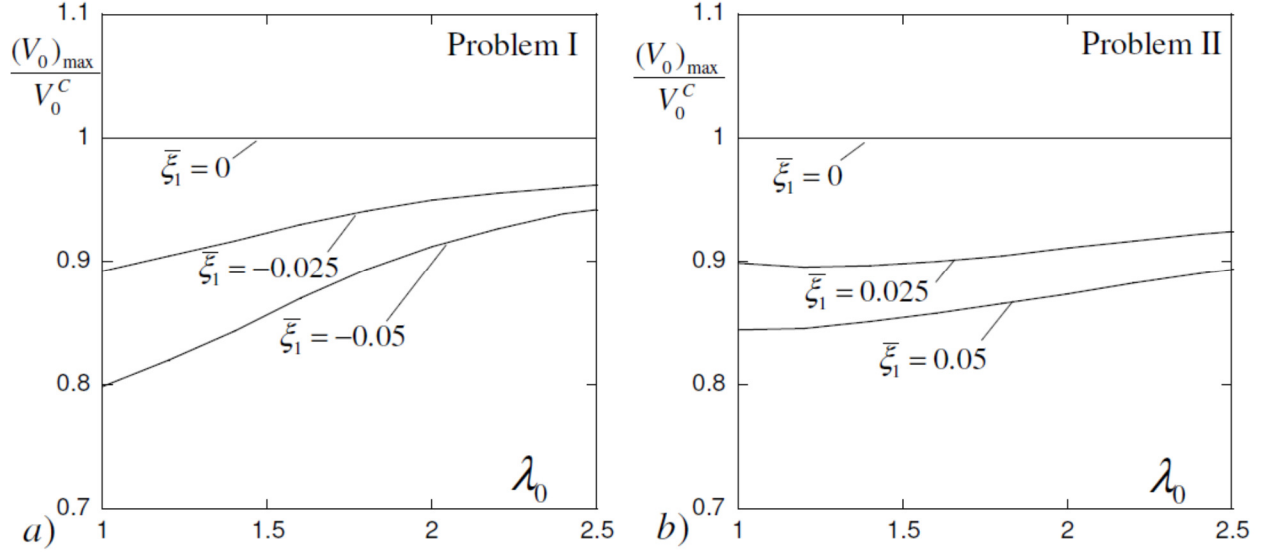
Fig. ESM-3 Imperfection-sensitivity of maximum voltage as a function of pre-stretch for Problem I in a) and for Problem II in b) for a perturbing force imperfection with amplitude $\bar{\xi}^{(1)}$.

Geometric and perturbing force imperfections in shape of surface modes:

Geometric imperfections with no pre-stretch

The reader is referred to Cao and Hutchinson (2012) for a systematic derivation of the modification of the energy functional that accounts for an initial stress-free surface undulation of the type considered here when there is no pre-stretch. The imperfection from (4.13) is

$$\bar{u}_2(x_1, 0) = \ell \sum_{i=1}^{N} \bar{\xi}_i^{G} \cos(2\pi i x_1 / \ell) \qquad \text{(ESM-25)}$$

In the absence of pre-stretch, the lowest order contribution to the terms in the energy functional $\Delta\Psi$ that are independent of Ω are of order $\xi^2 \bar{\xi}$ which are neglected compared to the contributions from the terms in $\Delta\Psi$ which are linear in Ω and quadratic in u. These are of. The lowest order contributions, which are of order $\xi\bar{\xi}$, can be obtained directly using terms quadratic in u and linear in Ω in either (4.1) or (4.4) by substituting $u_2 = \sum_{j=1}^{N} (\xi_j + \bar{\xi}_j) u_2^{(j)}$ into these expressions. The terms quadratic in $\bar{\xi}$ can be ignored because they do not contribute to the

variational equation. The lowest order imperfections terms are those of form $\Omega\xi\bar{\xi}$.
Alternatively, substitute u_2 into $-\Omega G_2(u)$ in (4.16), disregarding $-\Omega G_2(\bar{u})$ which does not
contribute to the variational equations, to obtain the additional term in (4.16):

$$-2\Omega_C \sum_{j=1}^{N} \xi_j G_{11}(u^{(j)},\bar{u}) = -\pi\mu\ell^2 \, \Omega_C \sum_{j=1}^{N} j\xi_j\bar{\xi}_j^G \qquad\qquad \text{(ESM-26)}$$

and, thus for the geometric imperfection, $\bar{a}_j = -2j$.

The error in the bifurcation result has some influence on the results presented in the
original paper for Problems I and II with imperfections and no pre-stretch, but the influence is
relatively minor. Qualitatively, the discussion of role of the geometric imperfections in the
original paper still holds and will not be revised. The main conclusion is that Problem I involves
surface deformations of the layer which are folds, or open crease-like modes, which probe
downward towards the other electrode. For Problem II, the surface deformation is a ridge-like
mode which is pulled toward the electrode above. With no pre-stretch, both problems are
strongly sensitive to geometric imperfections.

Perturbing force imperfections with or without pre-stretch

Identifying the contribution of the perturbing force/area distribution introduced in (4.15)
to the energy functional $\Delta\Psi$ is more straightforward than that for geometric imperfections. The
perturbing force/area distribution on the top surface of the layer, $p(x_1)$, is regarded as prescribed
and periodic with wavelength ℓ. Thus, the potential energy contribution of the perturbing force
imperfection to the periodic sector under consideration is $\Delta U = -\int_{-\ell/2}^{\ell/2} p(x_1)u_2(x_1,0)dx_1$. With

imperfection amplitudes $\bar{\xi}^{(j)}$ and $p(x_1) = \mu\sum_{j=1}^{N}\bar{\xi}^{(j)}\cos(jkx_1)$, the lowest order potential energy
contribution due to the imperfection is

$$\frac{\Delta U}{\pi\Omega_C\mu\ell^2/2} = -\frac{1}{\pi\Omega_C}\sum_{j=1}^{N}\xi^{(j)}\bar{\xi}^{(j)} \equiv \sum_{j=1}^{N}\bar{a}_j\xi^{(j)}\bar{\xi}^{(j)}$$

and this is the contribution included in ESM-21.

References

Hutchinson, J.W., 2013. The role of nonlinear substrate elasticity in the wrinkling of thin films, Phil. Trans. R. Soc. A 37120120422.

Visual Numerics, Inc., U., 1994. IMSL numerical analysis software.

Zang, J., Zhao, X., Cao, Y., Hutchinson, J. W., 2012. Localized ridge wrinkling of stiff films on compliant substrates. J. Mech. Phys. Solids, 60, 1265-1279.